Expression of Adrenomedullin and Its Receptor during Embryogenesis Suggests Autocrine or Paracrine Modes of Action

LUIS M. MONTUENGA, ALFREDO MARTÍNEZ, MAE JEAN MILLER, EDWARD J. UNSWORTH, AND FRANK CUTTITTA

Biomarkers and Prevention Research Branch, National Cancer Institute (L.M.M., A.M., M.J.M., F.C.), Rockville, Maryland 20850; the Department of Histology and Pathology, University of Navarra (L.M.M.), Pamplona, Spain; and the Center for Biologics Evaluation and Research, United States Food and Drug Administration (E.J.U.), Bethesda, Maryland 20892

ABSTRACT

The present study reports the developmental patterns of expression of adrenomedullin (AM) in rat and mouse embryos. AM is a novel multifunctional peptide recently isolated from a human pheochromocytoma, which has been shown to promote growth in a variety of mammalian cell lines. We have applied several techniques to investigate the localization of both the AM peptide and its receptor throughout development. Immunocytochemical detection has been performed using different specific antibodies against AM and its gene-related peptide pro-AM N-terminal 20 peptide. *In situ* hybridization showed the localization of the messenger RNAs for AM and its receptor. Western blot analysis together with reverse transcription-PCR gave further support to the localization of AM and its receptor in a variety of embryonic tissues. The localization of the receptor

paralleled that of AM itself, suggesting an autocrine or paracrine mode of action. The spatio-temporal pattern of expression of AM in cardiovascular, neural, and skeletal-forming tissues as well as in the main embryonic internal organs is described. The primitive placenta, especially the giant trophoblastic cells, shows high levels of AM and AM receptor. The heart is the first organ that expresses AM during development. The kidney, lung, and developing tooth, in which epithelial-mesenchymal interactions are taking place, show specific patterns of AM expression. In several regions of the embryo, the patterns of AM expression correspond to the degree of differentiation. The possible involvement of AM in the control of embryonic invasion, proliferation, and differentiation is discussed. (*Endocrinology* **138:** 440–451, 1997)

ADRENOMEDULLIN (AM) is a multifunctional peptide that has been identified from extracts of human pheochromocytoma (18). It is comprised of 52 amino acids and shows slight structural homology with calcitonin gene-related peptide (CGRP). Initial characterization demonstrated AM as a potent mediator of hypotension when injected iv into rats (18). AM and its gene-related peptide, proadrenomedullin N-terminal 20 peptide (PAMP), are the two known bioactive amidated peptides generated by posttranslational enzymatic processing of the 185-amino acid prepro-AM molecule (19). AM elevates intracellular cAMP levels in several cell types, and a receptor for AM (AM-R) has recently been cloned and sequenced (16). PAMP has no sequence homology with AM or CGRP and seems to act via a different receptor system (30). The expression of AM has been shown in a variety of adult rat, human, and porcine tissues, including heart, adrenals, brain, kidney, pancreas, aorta, lung, and brain- and lung-derived tumors (10, 23, 24, 31).

Apart from the vasorelaxant effect, several other functions have been reported for this peptide hormone. AM has been implicated in the regulation of renal function by means of its potent natriuretic and diuretic properties (14), has bron-

chodilatory effects (15), and inhibits the release of aldosterone, ACTH, and insulin (24, 28). Recent data suggest the involvement of AM in the regulation of growth. AM stimulates DNA synthesis and cell proliferation of Swiss 3T3 fibroblasts acting via the elevation of intracellular cAMP (32). Low concentrations (10–100 nM) of AM induced the cell cycle progression from G0 to G1 phase and the expression of c-*fos* messenger RNA (mRNA) in cultured rat aorta muscle cells (20). Moreover, our recent data show that numerous malignant cell lines express not only AM mRNA but also the mRNA for its receptor (25), suggesting the existence of an autocrine or paracrine type of growth regulation in human tumors. We also demonstrated that an inactivating anti-AM monoclonal antibody inhibits tumor cell growth in a dose-dependent manner, an effect that could be reversed by exogenous AM (25). Consistent with this proposed involvement in tumor growth control, AM has been found to be expressed in a variety of human malignancies of both neural and pulmonary lineage (23, 29).

An increasing number of peptides have been shown to be implicated in the long term modulation of growth and differentiation, not only in normal tissues but also in cancer, wound repair, and embryogenesis (3, 22, 26). These observations together with the recent data linking AM to the control of normal and tumor cells prompted us to investigate the possible role of AM in embryogenesis. Although the localization of AM in adult mammalian tissues and human neoplasms has been the object of some studies, the expres-

sion pattern during embryogenesis has not been reported. To gain further insight into the role of AM in embryonic development, we analyzed its expression in the mouse [embryonic days 8–16 (E8-16)] and the rat (E10-18) embryo. In the present study we show the expression of AM, AM-R, and PAMP during rodent embryogenesis by means of molecular, biochemical, and histochemical techniques.

Materials and Methods

Animals and tissue samples

Sections of Sprague-Dawley rat and NIH Swiss mouse staged embryos (Novagene, Madison, WI) were used. Adult female animals were caged with adult males overnight. The presence of a vaginal plug the following morning was designated day 0 of pregnancy. All specimens were fixed for 24 h in 4% buffered paraformaldehyde, embedded in paraffin, and sectioned at 7-μm thickness. Sections were mounted onto slides treated with Vectabond (Vector Laboratories, Burlingame, CA). For protein and mRNA extraction, pregnant rats (16 and 18 days after the morning when a vaginal plug was found) were used. Dams were obtained from SAIC (Frederick, MD; protocol 95/125) and killed by CO_2 overdose. The uterus was quickly removed and kept at 4 C while each embryo was dissected. Samples were kept at −80 C until extracted.

Antibodies

A previously reported, well characterized rabbit antiserum (no. 2343) was used to localize AM immunoreactivity in embryonic tissues (23). For the localization of PAMP, an antibody (no. 2463) was raised in rabbits against a synthetic peptide (P070) that represents the C-terminal eight amino acids of PAMP linked to a YY residue (YYWNKWALSR-NH$_2$). The P070 peptide was C-terminally amidated to conform with the C-terminus of native PAMP. The peptide was linked to key limpet hemocyanin via glutaraldehyde cross-linkage before immunization of the rabbits. The antibody was characterized for binding specificity using a solid phase RIA with [^{125}I]protein A as the detector. In brief, test peptides were passively absorbed onto individual wells (100 ng/well; overnight at 4 C) of a 96-well polyvinylchloride microtiter plate (Dynatech Laboratories, Chantilly, VA), after which the plate was coated with 1% BSA in PBS to minimize nonspecific binding. Test peptides included PAMP, P070, AM, CGRP, gastrin-releasing peptide, glucagon-like peptide-1, vasoactive intestinal peptide, IBE1, IBE2, substance P, arginine vasopressin, GRF, cholecystokinin, amylin, gastrin, oxytocin, calcitonin, αMSH, pancreatic polypeptide, peptide tyrosine-tyrosine, and *Tabanus atratus* hypotrehalosemic hormone (Peninsula Laboratories, Belmont, CA); BSA (Sigma Chemical Co., St. Louis, MO) was used as a negative control. Most of these test peptides were chosen because they are also C-terminally amidated. The antibody was tested at serial 2-fold dilutions ranging from 1:100 to 1:204,800. Very slight cross-reactivity was observed with glucagon-like peptide-1 and IBE2, and this was completely abolished when the antibody was preabsorbed with the peptide at 1 nmol/ml. The rest of the peptides tested gave negative results, except for PAMP and P070, which in our assay were readily recognized by the polyclonal antibody diluted up to 1:25,600.

Immunocytochemical technique

For the immunocytochemical localization of AM and PAMP in paraffin sections, the avidin-biotin complex technique was employed. Optimal dilution for anti-P072 was 1:1000, whereas the anti-P070 was used at a 1:600 dilution. After overnight treatment with the primary antiserum, sections were incubated with biotinylated goat antirabbit antiserum (Vector Laboratories) diluted 1:200. The sections were then treated with the avidin-biotin peroxidase complex (Vector Laboratories) diluted 1:100 in PBS. Peroxidase activity was demonstrated using diaminobenzidine-H$_2$O$_2$ as substrate. Finally, the sections were lightly counterstained with Gills' hematoxylin.

Solid phase absorption controls were carried out by preincubation (overnight at 4 C) of the primary antiserum with the equivalent peptide previously adsorbed to the wall of a polystyrene tube at a concentration of 10 μg/ml. Another negative control included the use of nonimmune swine serum as first layer and gave no immunocytochemical reaction.

Reverse transcription-PCR (RT-PCR)

The oligonucleotide primers were synthesized using a MilliGen/Biosearch 8700 DNA synthesizer (Millipore, Marlborough, MA). Primer sets for AM detection were as follows: sense (AM 250–270), 5'-AAG-AAG-TGG-AAT-AAG-TGG-GCT-3'; antisense (AM 523–542), 5'-TGT-GAA-CTG-GTA-GAT-CTG-GT-3'; and nested probe antisense (AM 430–450), 5'-TCT-GGC-GGT-AGC-GCT-TGA-CTC-3', with a predicted product of 293 bp. For human AM-R amplification, the following rat primers were selected from the published sequence (16): sense, AM-R-(476–497), 5'-AGC-GCC-ACC-AGC-ACC-GAA-TAC-G-3'; antisense, AM-R-(923–946), 5'-AGA-GGA-TGG-GGT-TGG-CGA-CAC-AGT-3'; and antisense probe, AM-R788-811, 5'-GGT-AGG-GCA-GCC-AGC-AGA-TGA-CAA-3', yielding a 471-bp product. Procedures for RT-PCR using these primers have been described previously (24). A Perkin-Elmer 9600 Thermocycler (Norwalk, CT) was used to amplify the samples for 35 cycles, with annealing temperatures of 55 and 60 C, respectively, for the ligand and its receptor. AM full-length probe was also generated by the PCR technique from normal human lung complementary DNA (cDNA; Clontech, Palo Alto, CA). PCR was performed using sense primer AM-(25–45) (5'-CCA-CTT-CGG-GCT-TCT-CAC-TGC-3') and antisense primer AM-(1304–1327) (5'-CAC-GCG-AAC-AAC-TTT-ACA-CCT-3') to obtain a 1303-bp product. Unique conditions were used during the PCR, with a (NH$_4$)$_2$SO$_4$-based buffer [10 mM (NH$_4$)$_2$SO$_4$, 10 mM KCl, 10 mM Tris-HCl (pH 8.4), 0.01% gelatin, and 0.1% Triton X-100] containing 3.75 mM MgCl$_2$. The annealing temperature was 55 C, and 35 cycles were performed. The PCR product was then cloned into the pCRII vector (Invitrogen, San Diego, CA) following the manufacturer's procedures.

In situ hybridization

Detection of the mRNA of both AM and its membrane receptor protein was performed using *in situ* hybridization. The full-length cDNAs for AM and AM-R (16) were ligated into the expression vectors pCRII and pcDNA1, respectively, and used to generate riboprobes. Both plasmids were linearized with *Eco*RV and *Bam*HI and used as a template to synthesize digoxigenin-labeled sense and antisense RNA transcripts. Hybridization was performed in a moist chamber at 46 C for 20 h in a 20-μl volume containing the probe. After stringency washes, visualization of digoxigenin was performed using digoxigenin detection kit (Boehringer Mannheim, Indianapolis, IN). Sense probes were used as controls.

Western blotting

To extract the proteins, the tissue samples were immersed in 2 × tricine sample buffer (with 8% SDS; Novex, San Diego, CA) containing a 1-μM final concentration of each of the following protease inhibitors: Pefabloc (Centerchem, Stamford, CT) and bestatin and phosphoramidon (Sigma Chemical Co.). The tissue was then homogenized, sonicated, and clarified by ultracentrifugation, and the final protein concentration was determined (BCA kit, Bio-Rad Laboratories, Richmond, CA). Tissue extracts were diluted to an approximate protein concentration of 35 μg/50 μl, heated to 95 C for 3 min, and loaded into the sample well.

Tissue extracts were electrophoretically separated on a gradient 10–20% tricine, SDS-PAGE gel (Novex) and run at 100 V for 2 h under reducing (5% β-mercaptoethanol) conditions. Five nanograms of synthetic AM were added to a separate well as a positive control. Transfer blotting was accomplished in the same apparatus equipped with a titanium plate electrode and transferred to a polyvinylidene difluoride membrane (Immobilon PVDF, Millipore) at 30 V for 3 h. The membrane was blocked overnight in 1% BSA-PBS, incubated for 1 h in a 1:1000 dilution of rabbit anti-AM (bleed 2343), washed three times in PBS, exposed to 1 × 10^6 cpm [^{125}I]protein A for 30 min at 4 C, washed six times in PBS, dried, and autoradiographed overnight at −80 C on Kodak XAR5 film (Eastman Kodak, Rochester, NY). The specificity control consisted of a duplicate membrane incubated in antigen-preabsorbed (10 nmol/ml) antiserum.

Results

Widespread expression of AM was identified throughout the embryonic development period of both mouse and rat. The brown immunocytochemical signal for both AM and PAMP and its intensity were modulated in a temporal fashion during embryogenesis. With the exception of the extraembrynic structures, low levels of AM and PAMP immunoreactivity were detected in the embryo at the beginning of organogenesis (mouse, E8-9; rat, E10-11), whereas these levels were dramatically increased during late organogenetic and early fetal growth periods (mouse, E13-16; rat, E15-17; Fig. 1, A–D). Table 1 summarizes the immunocytochemical detection of AM in the organogenetic period of the mouse. The distribution of AM- and PAMP-like immunoreactivities in the different tissues throughout the multiple stages of development of the two species studied were parallel; AM-like immunoreactivity was generally stronger than PAMP-like immunoreactivity (Fig. 1, D and E). The distribution for AM mRNA was coincident with the results obtained by immunocytochemical techniques. We also detected the mRNA of the AM-R protein in several tissues of the murine embryo at various stages.

RT-PCR was used to evaluate AM ligand and receptor mRNA in a variety of rat embryonic (E16 and E18) tissues (Fig. 2, A and B). The resulting 293- and 471-bp RT-PCR products for AM and AM-R mRNA were confirmed by Southern blotting with antisense nested probes. The majority of fetal tissues tested were shown to express AM and AM-R mRNA by RT-PCR, including the whole embryo, placenta, yolk sac, heart, lung, liver, brain, and gut. Tissue extracts from the same organs were examined for AM immunoreactivity by Western blot analysis using a previously characterized rabbit antiserum (23). Figure 2C illustrates the electrophoretic profile of the AM-like peptides identified. Molecular mass species of 18, 14, and 6 kDa were identified in tissue lysates and presumably represent AM precursor, processed intermediates, and the authentic peptide, respectively. The specificity of our immune detection assay was confirmed by an antibody absorption control that eliminated the specific bands.

Expression of AM in mouse development

Placenta and yolk sac. In the E8 embryo, a prominent immunocytochemical reaction was present in the primitive pla-
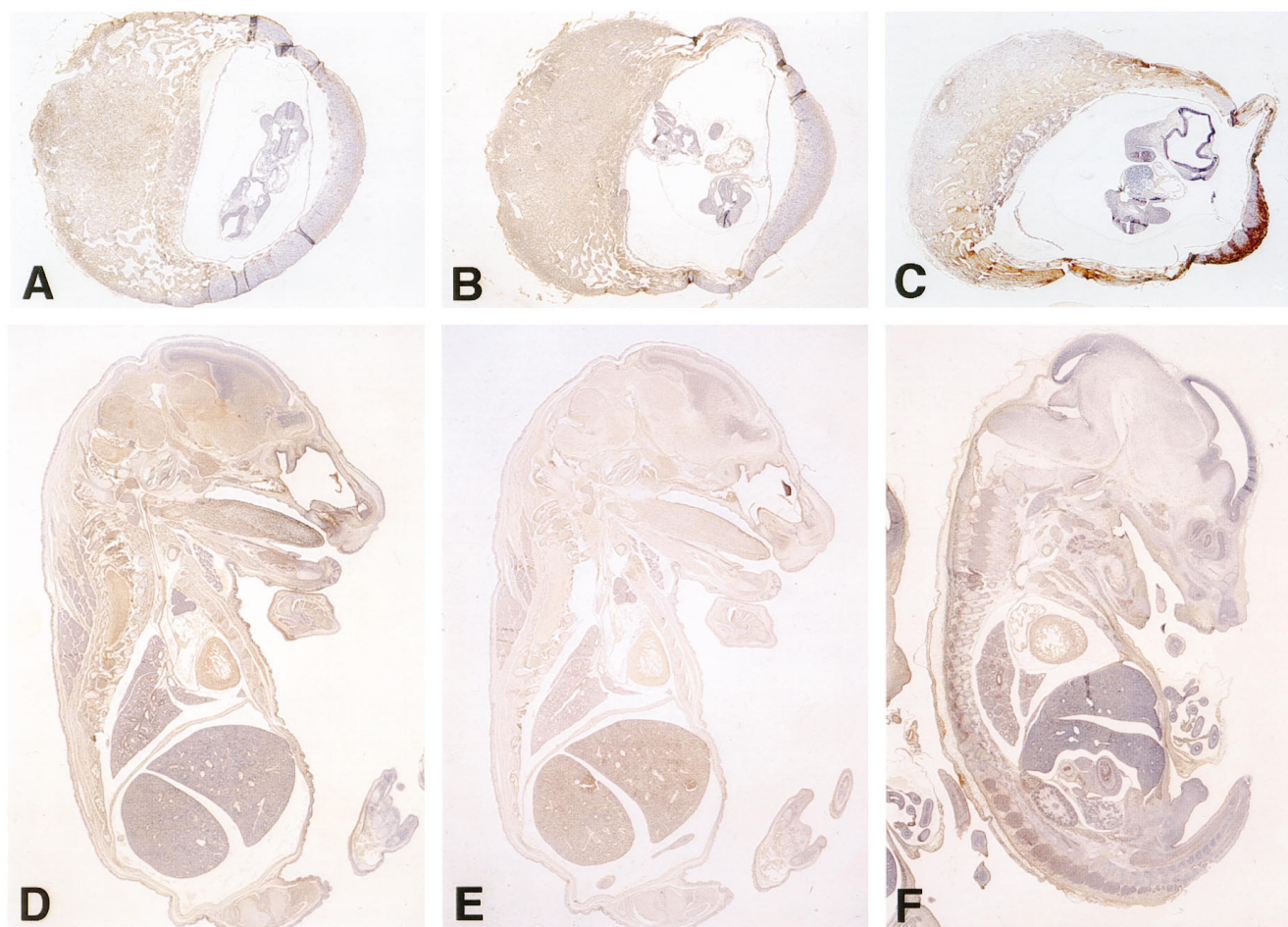

FIG. 1. Immunolocalization of AM and PAMP in early and late stages of mouse and rat development. AM and PAMP proteins were detected as described in *Materials and Methods*. A, Mouse E9. Primitive placenta and embryo immunostained for AM. B, Mouse E9. Primitive placenta and embryo immunostained for PAMP. C, Rat E11. Placenta and embryo immunostained for AM. D, Mouse E16. Section of the whole embryo immunostained for AM. E, Mouse E16. Section of the whole embryo immunostained for PAMP. F, Rat E16. Section of the whole embryo immunostained for AM. Note that placental tissues are positively stained in A, B, and C. Magnification: A, B, and C, ×10; D and E, ×5; F, ×6.

TABLE 1. Tissue distribution of immunohistochemically detectable adrenomedullin in mouse organogenesis

Tissue	Localization	E8	E9	E10	E11	E12	E13	E14	E15	E16
Heart		1	2	3	3	3	3	3	3	3
Arterial vasculature				1	2	2	2	2	2	2
Central nervous system	Brain	0	0	1	1	1	1	1	1	2
	Pituitary				1	ND	ND	1	1	1
	Choroid plexus			0/1	2	2	2	2	2	2
Peripheral nervous system	Spinal cord	0	0	1	1	1	2	2	2	2
	Dorsal root ganglia			0	0/1	1	2	2/3	3	3
Eye	Retina					0	0	0	0/1[a]	0/1[a]
Ear	Choclear epithelium				0	1	1	1	1/2	2
Skeletal structures	Skeletal muscle				0	1	2	2	2	2
	Precartilaginous blastema				0					
	Perichondrium				0	0	0	0/1	0	0
	Chondrocytes				0	1	2	2	2	2
	Hypertrophic cartilage							3	2	2
	Osteoblasts							2	2	3
Skin					1	2	2	2	2	2
Whisker follicles							1	2	2	2
Intestine	Epithelium						1	1	1	2
	Muscle fibers						1	2	2	2
Liver	Hepatocytes				0	0	0	1	1	1
	Megakaryocytes				1	1	1	1	1	1
Thymus	Cortex						ND	0	0	0
	Medulla						ND	0	1	1
Lung	Epithelial cells			0	1	1	1	1[b]/0[c]	1[b]/1[c]	0[b]/2[c]
	Mesenchyma			0/1	0	1	1	1	1	1
	Airway smooth muscle cells							0/1	1	1
Kidney	Metanephric duct derivatives						0	2	2	2
	Forming tubules						0	0	0	1
	Glomeruli					0	0	0/1[d]	1[d]	1[d]
Adrenal gland						1	2	2	2	2

Staining intensity is ranked from 0 (no staining) to 3 (very intense staining). ND, not determined.

[a] Outer neuroblastic layer.
[b] Prospective respiratory system.
[c] Prospective bronchial system.
[d] Glomerular capillary and mesangial tufts.

centa, whereas very low immunoreactive signal was found in the developing embryonic tissues (Fig. 1A and 3, A–C). Maternal decidual cells and the embryonic cells of the ecto-placental cone were intensely stained; the trophoblastic giant cells were particularly distinct (Fig. 3B) The cells of the chorionic plate were also immunoreactive for AM, but the intensity was lower than that for the other cell types examined. At the same stage, the visceral yolk sac, especially the vacuolated and microvillous border of the endodermal cells, was immunostained for AM. By nonradioactive *in situ* hybridization showing a blue/black precipitate, AM and AM-R mRNA were also localized to several cell types of the developing placenta, especially the giant trophoblastic cells (Fig. 3, D–H).

Cardiovascular system. On day 8, most of the cells of the developing mouse embryo were not stained, with the exception of the walls of the common atrial and ventricular chambers of the primitive heart, which were slightly immunoreactive for AM. In the E9 embryo, the cardiac tube was markedly immunostained with the antibodies against AM (Fig. 4A) and also expressed the receptor mRNA. The developing heart was the organ that showed higher levels of immunoreactivity throughout all stages of the mouse development. The myocytes of both atrial and ventricular walls, including the elaborate trabeculae formed around E10 in the ventricular chamber, were strongly stained for both AM and

AM mRNA (Fig. 4, B–D). The differentiating smooth muscle fibers found in the large arteries starting on E11 were strongly immunoreactive for AM (data not shown).

Nervous system. The neural tube, which was negative for AM during the preorganogenetic period (Fig. 1A), showed a detectable level of AM-like material by day 10. In this stage, the maturing cells of the ventral horn of the spinal cord showed AM-like immunoreactivity (Fig. 4E). As development continued, both the maturing postmitotic neural cells of the mantle layer and the neuropil of the marginal layer stained for AM in E11 embryos. On E12 and the following days, the difference between differentiated stained and less differentiated unstained areas of the central nervous system was more clear (Fig. 4F). From E12 on, specific groups of neurons positive for AM could be seen in the central nervous system, for example in the mantle layer of the spinal cord (Fig. 4F). mRNA for AM and for its receptor was shown in these neurons by *in situ* hybridization techniques (Fig. 4, G and H). Neural crest-derived dorsal root ganglia and their segmental nerve trunks became increasingly immunostained from E11-12 on (Fig. 4, I–K). In the earlier stages (Fig. 4I) only the trunks, but not neural cell bodies, were detectable with the anti-AM antibodies, whereas in E14 embryos, both neurons and nerve trunks were strongly stained (Fig. 4K). Throughout the rest of the development, the pattern of staining that was first seen in the nervous system on E12 remained, *i.e.* AM
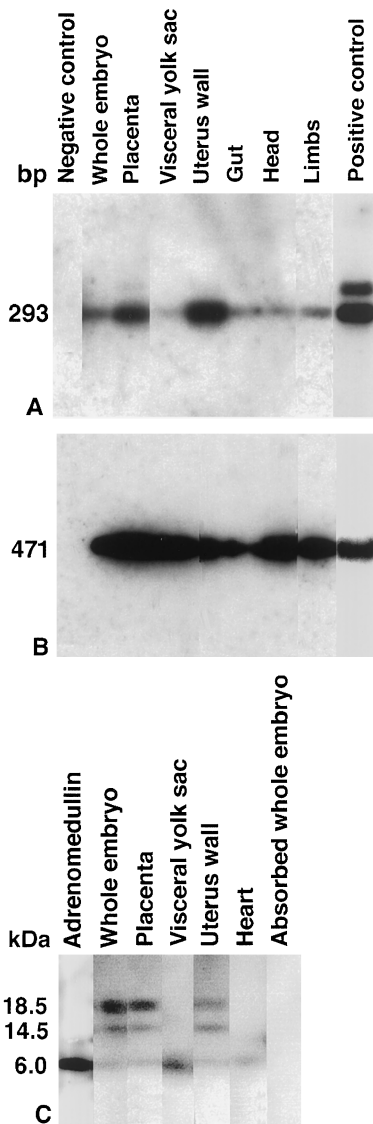
FIG. 2. Expression of AM and its receptor in different regions of the rat E16 embryo. Southern blot after RT-PCR for AM (A) and AM-R (B). C, Western blot using an antibody specific for AM (no. 2343). The bands of higher mol wt may correspond to unprocessed precursor. Absorption control was carried out for all tissues shown, but only one representative lane is included.

Skeletal and integumentary tissues. The presence of AM-immunoreactive material was observed at low levels in a diffuse pattern on groups of mesenchymal cells from E9 on. The mRNA for AM was present in the same cells at this stage. The expression of AM by the mesenchymal cells seems to follow precise patterns of spacio-temporal distribution, as the degree of staining of this tissue varied from one region to the other and during development. In the E12-13 stage, when the differentiation of the cartilaginous skeleton proceeds from condensed mesenchyma/precartilage toward more mature chondrocytic cells, AM-like material started to be expressed. Precondensing mesenchymal cells were immunocytochemically negative for AM (Fig. 4I). Maturing cartilage cells were increasingly positive from E13 on (Fig. 4J), and hypertrophic cartilage cells found from E15 were also highly stained (Fig. 4K). *In situ* hybridization showed that AM and AM-R mRNAs were clearly present in maturing chondrocytes (Fig. 4, G and H). Osteoblasts of the developing bone in the later stages of development were strongly immunoreactive for AM. During tooth development, AM-like expression could be observed on E15-16 in the condensing mesenchyme and the columnar cells of the inner layer of the enamel epithelium as well as in the underlying forming bone (Fig. 4L). After differentiation, the striated muscle cells were also immunoreactive for AM. This was particularly evident between E12 and E14, when the tongue elongated and increased in volume, and the striated muscle fibers differentiated from the myotubes (Fig. 1B). AM-like expression could be observed in the outer layer of the early skin, the periderm, from the E10 stage and was remarkably strong in the epidermal cells of the more differentiated skin on day 14 and throughout the developmental stages that followed (Fig. 4F). AM mRNA and the mRNA for the receptor could also be found by *in situ* hybridization (Fig. 4, G and H). The cells that form the cortex of the hair follicles were immunostained, whereas the mesenchyma that will form the papilla was negative (data not shown).

Embryonic internal organs. Apart from the strong immunostaining found in the heart throughout development, other internal organs expressed AM in the mouse embryo. In the gut, development progressed in a proximal to distal direction, so that at one time point different segments of the gut were at various stages of maturation. Initially, when the lumen of the gut was small and was lined by a pseudostratified columnar epithelium, no AM staining could be observed (Fig. 5A). In E13 embryos, a slight apical immunostaining was present in the epithelial cells that formed the inner lining of the midgut loops. As the gut matured, the peripheral mesenchyme differentiated toward smooth muscle, whereas the subepithelial mesenchymal tissue originated the lamina propria, muscularis mucosa, and submucosa. Prominent AM expression was found on E13 in the mesenchymal cells that will form the gut muscle layer. From E14 on, the presence of AM in the epithelium increased. On E16, the more differentiated simple columnar intestinal epithelium showed a marked expression of AM located mainly in the apical region of the enterocytes (Fig. 5B). On days 11–12, bilobed megakaryocytes expressing AM were particularly detectable in the developing liver (data not shown). Although the pan-

was localized to the neuropil, individual or grouped neurons within the central nervous system, and dorsal root ganglia. A certain segmental progression in the degree of staining of dorsal root ganglia could also be detected within a given stage. Slight immunoreactivity was observed in the Rathke's pouch on E11 and in the forming adenohypophysis in later stages of embryogenesis. Choroid plexi were also strongly immunostained for AM throughout development. In the eye, a discrete immunocytochemical signal was detected in the outer neuroblastic layer of the retina on E14-15. *In situ* hybridization showed that the mRNA for AM was present in the same cells. The lens epithelium and the lens fibers were stained with the antibodies against AM and, more strongly, against PAMP (data not shown).
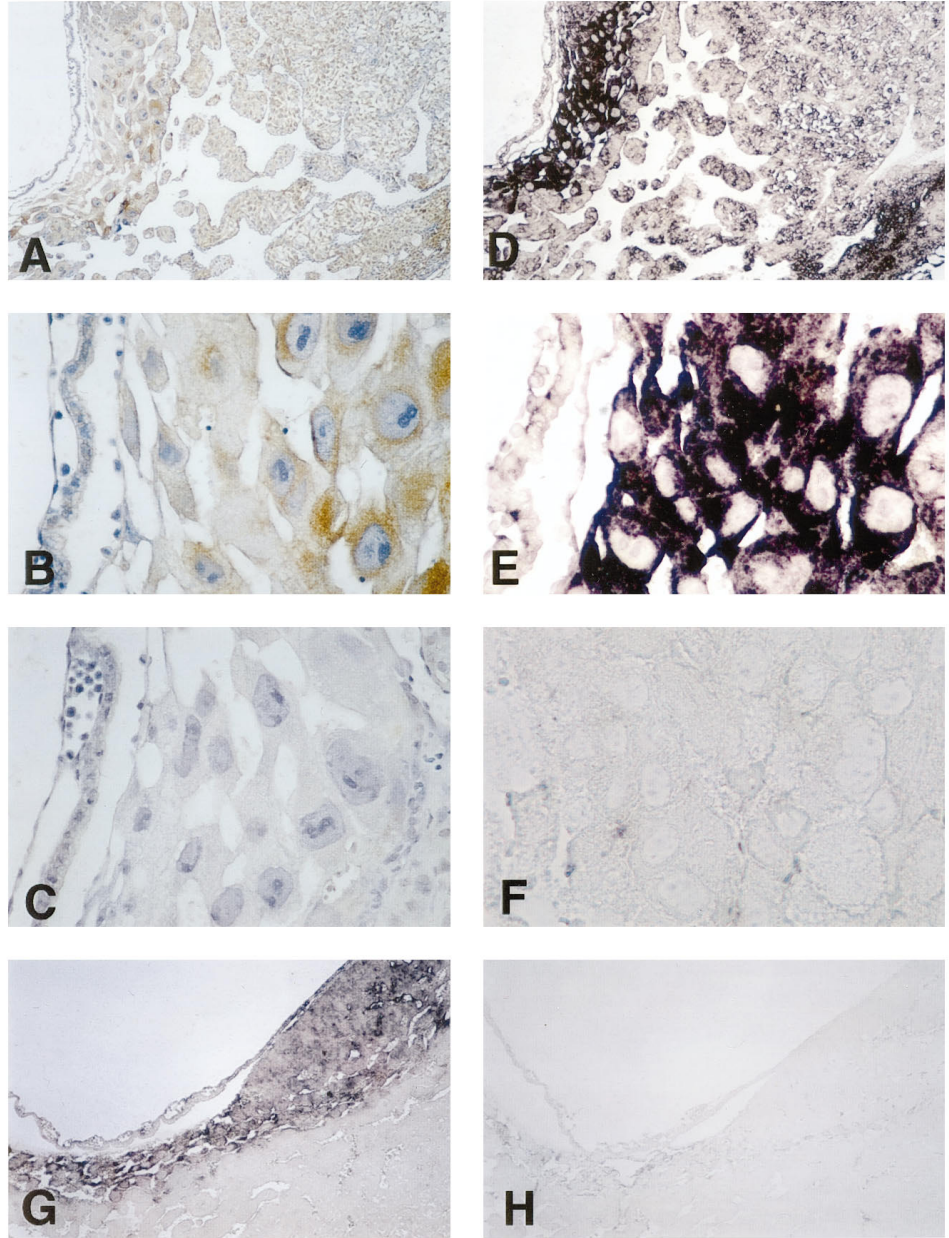
FIG. 3. Expression of AM and AM-R in the mouse primitive placenta on E9. A, Immunocytochemical detection of AM. B, Detail of giant trophoblastic cells immunostained for AM. C, Absorption control. D, Nonradioactive *in situ* hybridization for AM mRNA in the mouse placenta. E, Detail of the giant trophoblastic cells. F, Control using a sense probe. G, *In situ* hybridization for AM-R. H, Sense control. Magnification: A, D, G, and H, ×40; B, C, E, and F, ×200.

creatic primordia were initially negative for AM, on E14 a number of cells in the developing pancreatic ducts became immunoreactive for AM (Fig. 4D). The primordia of the endocrine islets that could be seen on E14 budding off the ducts were also intensely positive for AM (Fig. 4D). On E10.5, when the early lung bud was already formed, no expression was seen in the airway epithelium, and very little expression was found in the mesenchyme that surrounds it (Fig. 4E). On E11-12, the epithelium of the primordia of the bronchial tree showed increasing staining. Mesenchymal expression of AM in the lung was also increasingly present during these stages and was particularly notable in E13-14 embryos (Fig. 4F). In the lung of these embryos, the cells surrounding the developing bronchi that will differentiate into smooth muscle cells stained particularly strongly. Smooth muscle fibers of the forming arteries also expressed high levels of AM-immuno-

reactive material at this stage. By day 14, differentiation of the tubular epithelial system into the prospective bronchial system (central) and the prospective respiratory system (peripheral) had started. In E14-15 embryos. AM immunostaining was present in the latter epithelia and absent in the former. The pattern of staining reversed in later stages. In E15-16 embryos, a very clear staining was found in the epithelial lining of developing bronchi; the smooth muscle and the cartilage plates and rings of the bronchi and trachea were also stained (Fig. 5H). During the formation of the kidney, the first AM-expressing cells were found on E13-14 in the epithelium of the metanephric duct and later in the metanephric collecting tubules, but not in the mesenchyma, from which primitive glomeruli forms (Fig. 5, I and J). Slight AM immunoreactivity was found in the epithelium of the developing nephrons at the late S-shape body stage and in the final
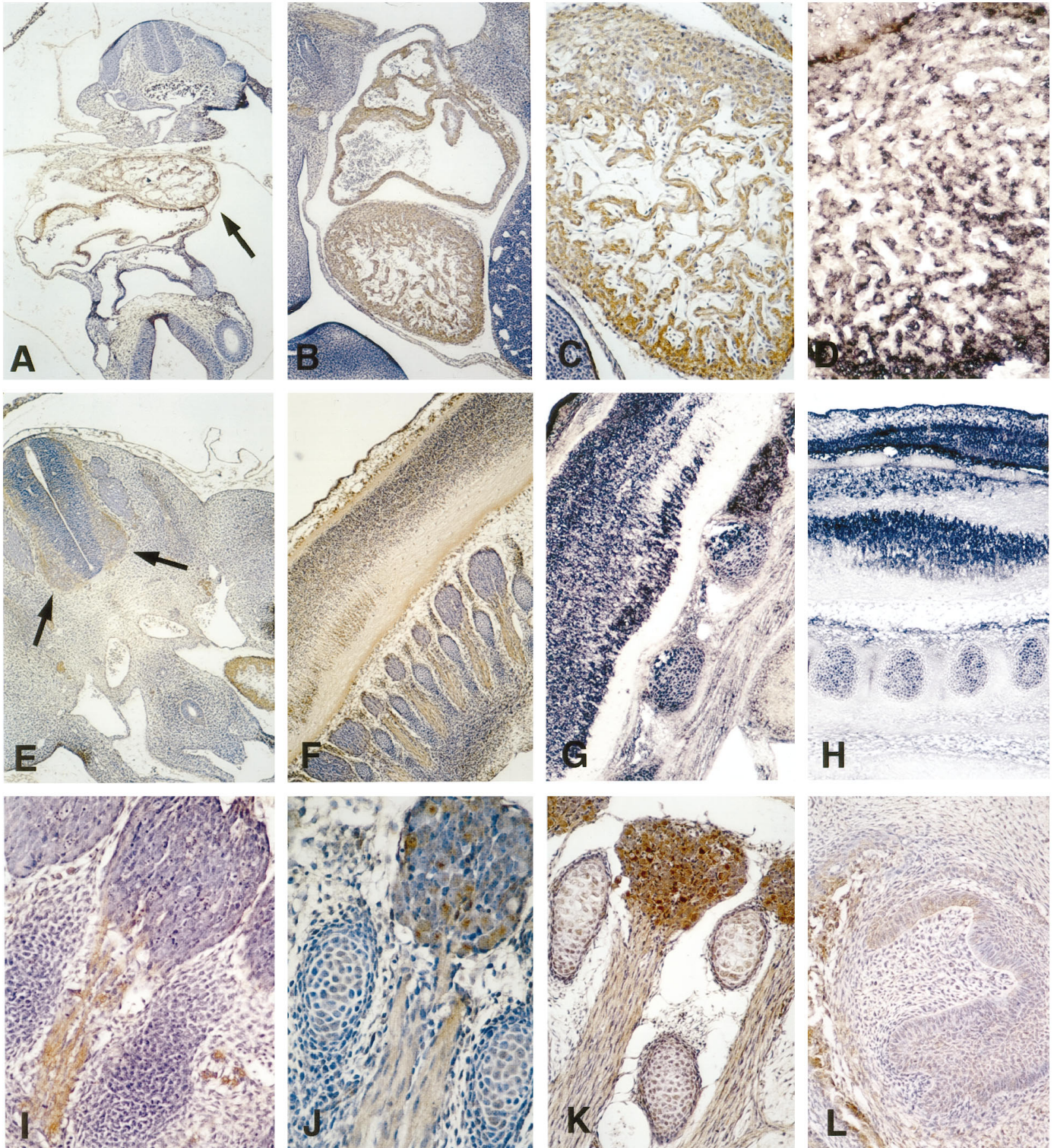
FIG. 4. Expression of AM and its receptor in several mouse tissues. Unless otherwise stated, figures show AM immunocytochemical detection. A, E9. Cardiac tube (*arrow*) and some mesenchymal cells are positive. B, E11. Atrium and ventricle are positive, whereas other organs are not stained. C, E11. Detail of heart. Cardiomyocytes but not endocardial cells are positive. D, E11. *In situ* hybridization for AM mRNA in a region similar to that shown in C. E, E10. Neural tube and related structures. Note the marginal layer of neural tube showing positive staining (*arrows*). F, G, and H, Longitudinal sections of the forming spinal cord and related structures. Note that skin, spinal cord neurons, dorsal root ganglia, and chondrocytes at vertebrae primordia express AM and its receptor. F, E12. G, E15. *In situ* hybridization for AM mRNA. H, E15. *In situ* hybridization for AM-R mRNA. I–K, Expression of AM during maturation of dorsal root ganglia and cartilage. I, E11. J, E12. K, E14. L, E15. Tooth primordium showing positive enamel epithelium and underlying forming bone. Magnification: A, B, E, F, G, and H, ×40; C, D, K, and L, ×100; J, ×200; I, ×300.
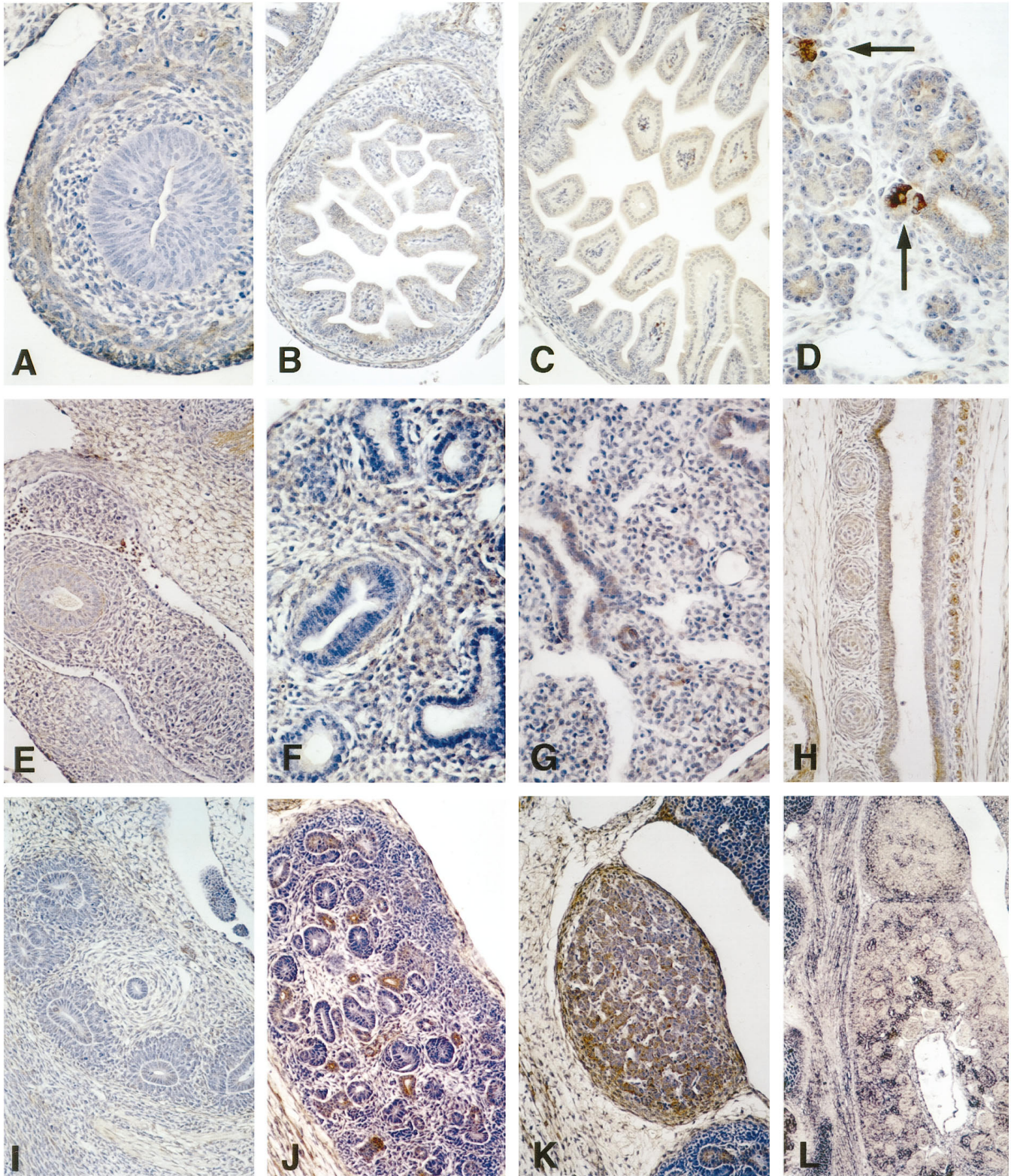
FIG. 5. Expression of AM in several internal organs of the developing mouse. Unless otherwise stated, figures show AM immunocytochemical detection. A–D, Digestive system. A, E13 gut. See differentiating smooth muscle immunostained for AM. B, E16 gut. C, E16 gut immunostained for PAMP. D, E16 pancreas. Note positive forming islets budding off the ducts (*arrows*). E–H, Respiratory tract. E, E11 lung primordium. F, E15 lung. Note positive mesenchymal staining. G, E16 lung. The epithelium of the airways is stained. H, E15 trachea. Epithelium, chondrocytes, and smooth muscle are immunostained. I–L, Kidney and adrenals. I, E12 kidney primordium. J, E14 kidney. Note that only some ducts (those derived from metanephric duct) are stained. K, E15 adrenal gland. L, E18. *In situ* hybridization to localize AM mRNA in the kidney. Only a subpopulation of ducts express AM mRNA. Note medullar and cortical staining in adrenal gland. Striated muscle and chondrocytes also express AM mRNA. Magnification: L, ×40; B, C, E, G, H, I, J, and K, ×100; A, D, and F, ×200.
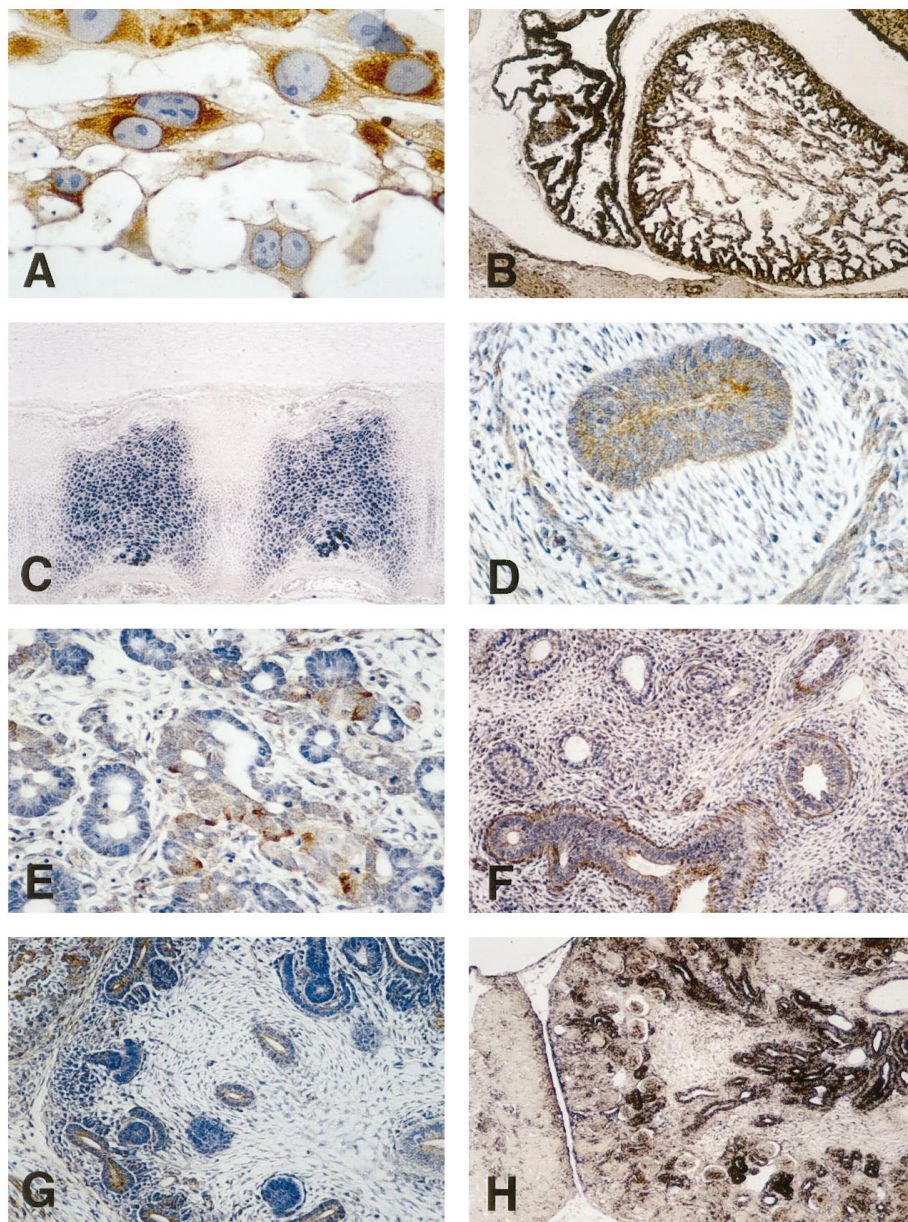
FIG. 6. Representative examples of expression of AM in rat development. Unless otherwise stated, figures show AM immunocytochemical detection. A, E11 giant trophoblastic cells. B, E15. *In situ* hybridization for AM in the heart. C, E18. *In situ* hybridization for AM receptor in mature and hyperplastic cartilage of the vertebrae. D, E16 stomach. Note that both epithelium and developing muscle layer are stained. E, E16 pancreas. Both endocrine and ductal cells are stained. F, E16 lung. Note positive staining on the forming smooth muscle surrounding the airways. G, E16 kidney. Metanephric duct and derived ducts are positively stained. Immunostained tissue of the adrenal gland can be seen in the left upper corner. H, E18. *In situ* hybridization for AM mRNA in the kidney. Apart from the ducts, some cells of the differentiating glomeruli express AM. Magnification: B and H, ×40; C and F, ×100; A, D, E, and G, ×200.

stages of development in the capillary and mesangial cell tufts of the developing glomeruli. The primordia of the adrenal glands expressed AM-immunoreactive material from E12-13 (Fig. 5K). Later in development, immunoreactivity in both the medulla and cortex of the adrenals could be found. The mRNA for AM followed the same pattern of distribution at this stage (Fig. 5L).

Expression of PAMP in mouse development

The expression of the AM gene-related peptide PAMP in the developing mouse was also studied. The pattern of appearance and distribution of PAMP was similar to that of AM (Figs. 1, C and D, and 5C). Nevertheless, the levels of immunocytochemical signal for PAMP were lower than those for AM.

AM and PAMP expression in the developing rat

The distribution of AM and PAMP immunoreactivity in the rat embryo was parallel to what we have described in the mouse when equivalent stages were compared (some representative examples can be found in Figs. 1, E and F, and 6). The pattern of appearance and distribution of AM immunoreactivity in the rat was very similar to that in the mouse, but occurred 1.5–2 days latter in development. Nevertheless, some differences were found between the two species. In the embryonic rat, endothelial cells expressed AM earlier and in a broader pattern than those in the mouse. AM-immunoreactive endothelial cells could be found as early as the E10 stage in the rat embryo and were also found in some very small vessels, such as those in developing glomeruli, on E16-17. The smaller blood vessels were less frequently

stained for AM in the developing mouse embryo. A clear AM staining for differentiated hepatocytes was found in the E17 rat embryo, which was less apparent in the equivalent stage of mouse development. In general, the later stages of development of rat embryos showed higher levels of AM immunoreactivity than the equivalent stages in the mouse. *In situ* hybridization for mRNA as well as for AM-R showed a parallel anatomical distribution. Our Western blot results (Fig. 2C) showed the presence of immunoreactive adrenomedullin in several organs of the E16 and E18 rat embryo. RT-PCR of isolated total mRNA also confirmed the presence of AM and AM-R message in the same stages of the rat embryo (Fig. 2, A and B).

Discussion

The results of our study strongly indicate that AM, AM-R, and PAMP are present in a large number of embryonic and extraembryonic cells and tissues in developing mouse and rat. Both the fetal and maternal tissues of the primitive placenta express high levels of these molecules. In the embryo proper, the onset of the increasing expression of AM-like peptide and mRNA occurs in the early organogenetic period in both species. Initially, it is restricted to limited regions of the embryo, but progresses to encompass most of the tissues and organs in the final stages of development. Our results suggest that this regulatory peptide may have an important function(s) in the complex biological processes taking place in embryogenesis.

To strengthen the conclusions drawn from the analysis of our immunocytochemical data concerning localization of AM, we have studied the distribution of PAMP encoded in the same precursor. The difference in intensity of immunostaining between AM and PAMP may reflect variations in intracellular levels of both peptides, possibly as the result of regulation of posttranslational processes. Alternatively, these differences may be due to the characteristics of the two antisera; in fact, solid phase RIA characterization studies (see *Materials and Methods*) showed that the antiserum used to detect PAMP (no. 2463) has lower titer than the one against AM (no. 2343). Moreover, we performed *in situ* hybridization studies using a specific probe to detect adrenomedullin mRNA. The three different approaches (localization of AM, PAMP, and their mRNA) show similar, if not identical, patterns of distribution. A further verification of our data comes from the simultaneous study of embryos of two species that also show a very analogous spatio-temporal pattern of AM expression. Finally, Western blot and RT-PCR analysis of total embryos and dissected late embryonic tissues were performed. Our biochemical results also show that both adrenomedullin and its receptor are present in different organs during development.

In general, the organs that express AM during murine development correspond to those described for adults, determined by RIA, Northern blot, and immunocytochemistry (10, 11, 23), with heart and adrenals showing higher levels of expression in both cases. Nevertheless, comparison of the distribution of immunocytochemical staining suggests that the relative AM expression in embryonic tissues in late organogenesis is even broader than that in adults.

The gene that codes for a membrane receptor protein specific for AM has recently been cloned from rat lung (16). Our results show a widespread distribution of the receptor in many tissues and organs of the developing mouse and rat. To date, the cellular distribution of this receptor has not been reported, with the exception of rat pancreas and lung (23, 24). The fact that the distribution of the AM receptor in most organs colocalizes with the ligand supports the hypothesis that AM may act locally in a short range autocrine or paracrine mode. Several other growth factors, such as platelet-derived growth factor (PDGF) or the several transforming growth factors-β (TGFβs), have been proposed to work in an autocrine/paracrine manner on the basis of a close juxtaposition, or even identity, of the cells expressing the receptors and the cells that secrete these factors (1, 4).

The formation of organs during embryogenesis is highly dependent on the sequential and time-regulated expression of a number of growth factors (26). The pattern of distribution of AM-like immunoreactivity and its mRNA during murine development is very similar to that of other well established peptide growth factors. The distribution of AM immunoreactivity shown in our study is very similar to that reported for the TGFβ isoforms 1, 2, and 3 in the E12-18.5 mouse embryos (2, 27), suggesting that AM and the TGFβs could be involved in analogous functions. AM distribution also shows some coincident locations with other active peptides such as PDGF, the fibroblast growth factors, insulin-like growth factors I and II, and the recently discovered cardiotropin, a member of the leukemia inhibitory factor/interleukin-6 family. On a comparative basis with the data available on the above-mentioned growth factors, AM seems to be the peptide that is expressed in a larger variety of cells and tissues throughout development, which suggests that this peptide is an important requirement for development to proceed in most organs.

An interesting finding is that AM is intensely expressed in tissues and organs where strong mesenchymal-epithelial interactions take place, such as kidney, lung, tooth primordia, and hair follicles. The expression of AM in these structures is tightly regulated and restricted to particular structures in a given developmental stage. In the kidney, for example, AM is initially expressed only in the ureteric bud-derived metanephric ducts. Later in development, the differentiating nephron tubules and the glomeruli tufts begin to express AM. Other growth factors, such as insulin-like growth factors I and II, TGFβ1 and -2, and PDGF are also expressed in the developing kidney in a very specific spatial and temporal pattern (8).

In adult mammals, AM has been shown to have multiple and diverse functions. A broad spectrum of functions, such as *in vivo* and *in vitro* regulation of embryonic cell proliferation, differentiation, and migration, is also a common feature for other thoroughly studied growth factors (for a review, see Ref. 26). Our results on the localization of AM and its receptor together with the available data on the diverse functions of AM have lead us to formulate the hypothesis that AM could be involved in the regulation of mammalian morphogenesis, possibly through the control of cell proliferation, differentiation, and migration.

Several reports have shown that AM acts as a true growth

factor in several normal and malignant tissues. The potent mitogenic effect of AM on embryonic mouse fibroblasts has been reported recently (32). AM also stimulates growth in tumor cell lines via an autocrine loop (25) and promotes cell cycle progression from the G0 to the G1 phase and the expression of c-*fos* mRNA in vascular smooth muscle cells (20). These reports coincide by showing a cAMP-dependent signal of transduction pathway effecting growth for AM. Interestingly, AM seems to act also as a suppressor of mitogenesis in cultured rat mesangial cells and vascular smooth muscle (5). This duality of regulatory functions could be due to the participation of different protein kinase isoforms in the cellular response to AM (12).

A functional relationship between the expression of AM and differentiation can be deduced by the anatomical distribution of AM immunoreactivity and mRNA. In many embryonic organs, AM expression seems to correlate with the onset and progression of the differentiation process. For example, in the formation of the cartilaginous templates that precede bone, AM and AM-R seem to be expressed in the more mature cell types in the chondrocyte lineage, including the hypertrophic cells, whereas the condensing mesenchymal cells that are present in the previous stages express very low, if any, levels of the peptide and its receptor. The expression of growth factors in the formation of cartilage has been the object of a number of studies (7). Interestingly, a relationship between cAMP and terminal differentiation and calcification of cultured chondrocytes has been clearly established (13), which could support the involvement of AM in the regulation of this process through its cAMP-dependent signal transduction system. Various other active factors that affect chondrocyte differentiation also increase the cAMP concentration in chondrocytes (17). The localization of AM, its mRNA, and the mRNA of its receptor to the growing skeletal structures and the fact that AM elicits its biological actions via the elevation of cAMP levels suggest an involvement of AM in embryonic chondrocyte maturation. Further investigation is required into the proper *in vitro* and *in vivo* models to clarify the exact role of AM in chondro- and osteogenesis. Another example in which the expression of AM seems to be associated with the degree of differentiation is neural tissue. Although in the early neural tube, neither immunocytochemical signal of AM nor mRNA of the ligand or the receptor is present, as development proceeds, AM starts to be expressed in many of the more mature and differentiated regions of the central nervous system. The expression of AM in the dorsal root ganglia neurons is also increased in the later stages of development, especially from the moment when most of the dorsal root ganglia neurons are probably formed (21).

Our immunocytochemical results as well as the data on localization of the mRNA of AM and its receptor consistently show that trophoblastic cells, in particular the giant trophoblastic cells, express AM and AM-R at high levels. A possible autocrine or paracrine loop that could regulate the physiology of this cell type is proposed. Murine giant trophoblast cells as well as their human counterparts share *in vivo* and *in vitro* invasive properties with malignant cells (33). The AM regulatory role on these cells could be similar to that of TGFβ, which is known to be produced by trophoblast cells and

seems to be involved in the regulation of trophoblast invasiveness via the induction of tissue inhibitor of metalloproteases and by decreasing collagenase IV activity (6). Invasiveness by trophoblastic cells is also regulated by leukemia inhibitory factor and epidermal growth factor via the stimulation of matrix metalloproteases and other proteinases (9).

In summary, our study has shown a widespread expression of the recently discovered multifunctional peptide AM, its receptor, and its gene-related peptide PAMP throughout the organogenetic stages of mouse and rat embryos. Based on the sites of expression and by analogy with other multifunctional growth factors for which functional studies have been performed, we propose that the AM regulatory system may play an important role in a variety of key processes in embryonic development, namely in the control of growth, differentiation, and invasion. Further functional evaluation, on the basis of our distributional study, will clarify the validity of our hypothesis.

Acknowledgments

References

1. **Akhurst RJ** 1994 The transforming growth factor β family in vertebrate embryogenesis. In: Nilsen-Hamilton M (ed.) Growth factors and signal transduction in development. Wiley-Liss Inc, New York, 97–122
2. **Akhurst RJ, Fitzpatrick DR, Fowlis DJ, Gatherer D, Millan FA, Slager H** 1992 The role of TGF-βs in mammalian development and neoplasia. Mol Reprod Dev 32:127–135
3. **Baserga R** 1994 Oncogenes and the strategy of growth factors. Cell 79:927–930
4. **Bowen-Pope DF, Seifert RA** 1994 Platelet-derived growth factor in development. In: Nilsen-Hamilton M (ed.) Growth factors and signal transduction in development. Wiley-Liss Inc., New York, 51–73
5. **Chini EN, Choi E, Grande JP, Burnett JC, Dousa TP** 1995 Adrenomedullin suppresses mitogenesis in rat mesangial cells via cAMP pathway. Biochem Biophys Res Com 215:868–873
6. **Graham CH, Lala PK** 1991 Mechanisms of control of trophoblast invasion *in situ*. J Cell Physiol 148:228–234
7. **Hall BK, Miyake T** 1995 Divide, accumulate, differentiate: cell condensation in skeletal development revisited. Int J Dev Biol 39:881–893
8. **Hammerman MR** 1995 Growth factors in renal development. Sem Nephrol 15:291–299
9. **Harvey MB, Leco KJ, Arcellana-Panlilio MY, Zhang X, Edwards DR, Schultz GA** 1995 Proteinase expression in early mouse embryos is regulated by leukemia inhibitory factor and epidermal growth factor. Development 121:1005–1014
10. **Ichiki Y, Kitamura K, Kangawa K, Kawamoto M, Matsuo H, Eto T** 1994 Distribution and characterization of immunoreactive adrenomedullin in human tissue and plasma. FEBS lett 338:6–10
11. **Ichiki Y, Kitamura K, Kangawa K, Kawamoto M, Matsuo H, Eto T** 1995 Distribution and characterization of immunoreactive adrenomedullin in porcine tissues, and isolation of adrenomedullin [34–52] from pocine duodenum. J Biochem 118:765–770
12. **Ishizuka J, Towsend CM, Bold RJ, Martínez J, Rodríguez M, Thompson JC** 1994 Effects of gastrin on 3′,5′-cyclic adenosine monophosphate, intracellular calcium, and phosphatidylinositol hydrolysis in human colon cancer cells. Cancer Res: 54:2129–2135
13. **Jikko A, Murakami H, Yan W, Nakashima K, Ohya Y, Satakeda H, Noshiro M, Kawamoto T, Nakamura S, Okada Y, Suzuki F, Kato Y** 1996 Effects of cyclic adenosine 3′,5′-monophosphate on chondrocyte terminal differentiation and cartilage matrix calcification. Endocrinology: 137:122–128
14. **Jougasaki M, Wei CM, Aarhus LL, Heublen DM, Sandberg SM, Burnett JC** 1995 Renal localization and actions of adrenomedullin: A natriuretic peptide. Am J Physiol 268:F657–F663
15. **Kanazawa H, Kurihara N, Hirata K, Kudoh S, Kawagushi T, Takeda T** 1994 Adrenomedullin, a newly discovered hypotensive peptide, is a potent bronchodilator. Biochem Biophys Res Co 205:251–254
16. **Kapas S, Catt KJ, Clark JL** 1995 Cloning and expression of cDNA encoding a rat adrenomedullin receptor. J Biol Chem 270:24344–25347
17. **Kato Y, Koike T, Iwamoto M, Kinoshita M, Sato K, Hiraki Y, Suzuki F** 1988

Effects of limited exposure of rabbit chondrocyte cultures to parathyroid hormone and dibutyryl adenosine 3′,5′-monophosphate on cartilage -characteristic proteoglycan synthesis. Endocrinology 107:1991–1997

18. **Kitamura K, Kangawa K, Kawamoto M, Ichiki Y, Nakamura S, Matsuo H, Eto T** 1993 Adrenomedullin: a novel hypotensive peptide isolated from human pheochromocytoma. Biochem Biophys Res Co 192:553–560

19. **Kitamura K, Kangawa K, Ishiyama Y, Washimine H, Ichiki Y, Kawamoto M, Minamino N, Matsuo H, Eto T** 1994 Identification and hypotensive activity of proadrenomedullin N-terminal 20 peptide (PAMP). FEBS lett 351:35–37

20. **Kobayashi S, Shikasho T, Nishimura J, Kureishi Y, Kanaide H** 1995 Adrenomedullin stimulates the cell cycle progression and the expression of c-fos messenger RNA in vascular smooth muscle cells in primary culture. Circulation 92:I-694 (Abstract #3335)

21. **Lawson SN, Caddy KWT, Biscoe TJ** 1974 Development of rat dorsal root ganglion neurones. Studies on cell birthdays and changes in mean cell diameter. Cell Tiss Res 153:399–413

22. **Martin P, Hopkinson-Woolley J, McCluskey J** 1992 Growth factors and cutaneous wound repair. Progress in Growth Factors Research 4:25–44

23. **Martínez A, Miller MJ, Unsworth EJ, Siegfried JM, Cuttitta F** 1995 Expression of adrenomedullin in normal human lung and in primary tumors. Endocrinology 136:4106–4112

24. **Martínez A, Weaver C, Lopez J, Bhathena SJ, Elsasser TH, Miller MJ, Moody TW, Unsworth EJ Cuttitta F** 1996 Regulation of Insulin secretion and blood glucose by adrenomedullin. Endocrinology 137:2626–2632

25. **Miller MJ, Martínez A, Unsworth EJ, Thiele CJ, Moody TW, Cuttitta F** 1996 Adrenomedullin: expression in human tumor cell lines and its potential role as an autocrine growth factor. J Biol Chem 271:23345–23351

26. **Nilsen-Hamilton M** 1994 Growth Factors and signal transduction in development. Wiley-Liss Inc., New York

27. **Pelton RW, Saxena B, Jones M, Moses HL, Gold LI** 1991 Immunohistochemical localization of TGFβ1, TGFβ2, TGFβ3, in the mouse embryo: expression patterns suggest multiple roles during embryonic development. J Cell Biol 115:1091–1105

28. **Samson WK, Murphy T, Schell DA** 1995 A novel vasoactive peptide, adrenomedullin, inhibits pituitary adrenocorticotropin release. Endocrinology 136:2349–2352

29. **Satoh F, Takahashi K, Murakami O, Totsune K, Sone M, Ohneda M, Abe K, Miura Y, Hayshi Y, Sasano H, Mour T** 1995 Adrenomedullin in human brain, adrenal-glands and tumor-tissues of pheochromocytoma, ganglioneuroblastoma and neuroblastoma. J Clin Endocr Metab 80:1750–1752

30. **Shimosawa T, Ito Y, Ando K, Kitamura K, Kangawa K, Fujita T** 1995 Proadrenomedullin NH2-Terminal 20-peptide, a new product of the adrenomedullin gene, inhibits norepinephrine overflow from nerve-endings. J Clin Invest 96:1672–1676

31. **Washimine H, Asada Y, Kitamura K, Ichiki Y, Hara S, Yamamoto Y, Kangawa K, Sumiyoshi A, Eto T** 1995 Immunohistochemical identification of adrenomedullin in human, rat and porcine tissue. Histochem Cell Biol: 103:251–254

32. **Withers DJ, Coppock HA, Seufferlein T, Smith DM, Bloom SR, Rozengurt E** 1996 Adrenomedullin stimulates DNA synthesis and cell proliferation via elevation of cAMP in Swiss 3T3 cells. FEBS Lett 378:83–87

33. **Yagel S, Parhar RS, Jeffrey JJ, Lala PK** 1988 Normal nonmetastatic human trophoblast cells share *in vitro* invasive properties of malignant cells. J Cell Physiol 136:455–462